ECRONICON OPEN ACCESS

PHARMACEUTICAL SCIENCE
Research Article

DSC-FTIR Combined Approaches Used to Simultaneously Prepare/Determine the Amorphous Solid Dispersions of Indomethacin/Soluplus in Real-time

Hong-Liang Lin[1], Ying-Ting Chi[1], Yu-Ting Huang[1], Chi-Yu Kao[1] and Shan-Yang Lin[1]*

Department of Biotechnology and Pharmaceutical Technology, Yuanpei University of Medical Technology, Taiwan

***Corresponding Author:** Shan-Yang Lin, Department of Biotechnology and Pharmaceutical Technology, Yuanpei University of Medical Technology, Yuanpei street, Hsin Chu 30015, Taiwan.

Received: June 22, 2015; **Published:** September 03, 2015

Abstract

A simultaneous differential scanning calorimetry-Fourier transform infrared (DSC-FTIR) microspectroscopy was first used to directly prepare and detect the amorphous information of indomethacin (IMC) in the γ-IMC/Soluplus physical mixture with or without solvent evaporation via two consecutive heating-cooling cycles via a one-step procedure. The thermal-induced phase transformation of Soluplus or different IMC polymorphs was also studied by DSC analytical method and this one-step DSC-FTIR combined approach. The result of this study indicates that the amorphous IMC exhibited three characteristic IR peaks at 1710, 1683 and 1591 cm^{-1} with a shoulder at 1735 cm^{-1}. Four transitions in the three-dimensional FTIR spectral contour map of amorphous IMC were observed, and finally transformed to α-IMC and γ-IMC, in agreement with the changes in DSC curve of the amorphous IMC. The intramolecular hydrogen bonding occurred in the carboxylic acid dimers of γ-IMC structure was gradually dissociated in the γ-IMC/Soluplus physical mixture via the first-heating run by using this one-step DSC-FTIR combined approach. After the first heating-cooling cycle, the amorphous formation of IMC in the IMC/Soluplus amorphous solid dispersion (ASD) system was successfully produced due to the appearance of both characteristic IR peaks at 1682 and 1594 cm^{-1} for the amorphous IMC formed. However, this IMC/Soluplus ASD system formed only showed a consistent three-dimensional FTIR spectral contour map in the second-heating run without any changes. On the other hand, the γ-IMC/Soluplus physical mixture after solvent evaporation revealed similar consistent three-dimensional FTIR spectral contour maps after first and second heating-cooling runs, since the IMC/Soluplus ASD system was already formed after solvent evaporation. Since the DSC-FTIR combined technique gives spectroscopic and thermodynamic information, both the induction and identification of the amorphous IMC formation and phase transition of samples could be simultaneously obtained. The present study clearly evidences that this simultaneous DSC-FTIR combined approach was not only capable of preparing the IMC/Soluplus ASD system from physical mixture but also capable of determining the amorphous formation of IMC in the IMC/Soluplus ASD system in real-time via a one-step procedure.

Keywords: *Indomethacin (IMC); Soluplus; Amorphous IMC; Solid dispersion; DSC-FTIR*

Abbreviations: APIs: Active pharmaceutical ingredients; ASD: Amorphous solid dispersion; BCS: Biopharmaceutics Classification System; DSC-FTIR: Differential scanning calorimetry-Fourier transform infrared spectroscopy; HME: Hot melt extrusion; IMC: Indomethacin; KBr: Potassium bromide; MCT: Mercury-cadmium telluride (MCT)

Introduction

More than 40-60% of commercially available active pharmaceutical ingredients (APIs) have been reported to have poor water solubility problems, leading to the limitation of their efficacy [1-2]. The FDA's Biopharmaceutics Classification System (BCS) is based on the work of Prof. Amidon and coworkers to predict *in vivo* performance of drug products from *in vitro* measurements of solubility and permeability [3-5]. In order to solve the problems of poorly water soluble and low dissolution rate of many APIs, various pharmaceutical technologies

have been extensively investigated and developed in both academia and industry, including micronization, salt formation, micellar solubilization, cyclodextrin complexation, solid dispersion and others, by combining with different specific processing techniques [5-8].

Recently, solid dispersion is one of the most promising technologies in pharmaceutical industry to improve the oral bioavailability of poorly water-soluble drugs [9-12]. Solid dispersions of drugs can be easily prepared by different methods to render and maintain the drug in the amorphous state and/or adequately dispersing it within a carrier matrix. Since the amorphous form of APIs has higher solubility than its crystalline form, thus the use of amorphous from may provide an opportunity to potentially improve solubility and bioavailability of APIs [12-13]. In the formulation design by using solid dispersion techniques, it is possible to choose a suitable polymeric carrier to modify the molecular mobility, relaxation times and intermolecular interaction of APIs in the solid dispersions [14-15].

Although amorphous APIs have an advantage to enhance the bioavailability of poorly soluble APIs, the amorphous form of API is always in a highly metastable state to drive towards crystallization during manufacturing or storage for losing its original advantages [9, 16-17]. Thus, how to maintain the amorphous state of API in the solid dosage form is the major challenge in formulation design. Several solid dispersions by incorporating the poorly water-soluble drugs into different water-soluble polymers with available methods have been widely investigated [12, 17-18]. A proper selection of the polymer carrier is an important key factor in the formulation development of solid dispersions. The types of water-soluble polymer carriers play a more critical role in affecting the physical stability of amorphous form of drugs during *in vitro* and *in vivo* conditions [19-21].

Soluplus® is a new developed amorphous polyvinyl caprolactam - polyvinyl acetate - polyethylene glycol graft copolymer, which consists of 57% vinyl caprolactam, 30% vinyl acetate and 13% PEG 6000 [22]. Soluplus has been classified as a member of the fourth generation of solid dispersion carriers to enhance the highest degree of dissolution of poorly water-soluble drugs and also to stabilize these drugs in the solid dispersions [10]. Particularly, as compared with other classical solubilizers, Soluplus has bifunctional character to act as a matrix polymer for solid dispersions and an active solubilizer through micelle formation in water [22-24]. Since the low glass transition temperature (*Tg*) value (approximately 70°C) of Soluplus, it can be easily used to prepare amorphous solid dispersion (ASD) system by thermal and/or solvent based methods [22, 25-26]. It has been reported that Soluplus might effectively enhance the absorption of different BCS class II compounds [22, 24-27].

Indomethacin (IMC) has been described as a typical BCS class II drug with a low bioavailability when administered orally, due to its poorly water-soluble property [3]. The water-insoluble property of IMC may increase the incidence of irritating side effects on the gastrointestinal tract after prolonged contact time with the mucosa [28]. In addition, IMC has been recently proposed to act as an effective agent for decreasing the risk of various types of cancers including human breast cancer and esophageal cancer cell lines [29-30], suggesting a possible future potential of IMC. Thus numerous attempts have been made to select IMC as a model drug for preparing an amorphous form of IMC to enhance its water solubility and dissolution rate from various solid dosage forms [31-33]. However, the recrystallization of amorphous IMC under different temperatures and humidities has also been reported to alter its *in vitro* water solubility and *in vivo* bioavailability [34-36].

Nowadays, hot melt extrusion (HME) technique has been considerably established as a novel tool to prepare the ASD system [12, 37-39], in which the heat is applied to the materials for controlling its viscosity and enabling it to flow through the die during HME process, and followed by instant cooling of the melt to form solid dispersions. This demonstrates that the thermal processing plays an important role in the preparation of ASD system. During the HME process, not all polymers can be used to induce the amorphization of drugs in polymer blends. Thus the selection of a proper polymer carrier is a major issue in the formulation design of ASD system, in which Soluplus has been especially designed for HME technology [22-23, 25-27].

In our previous studies, we had used a unique differential scanning calorimetry-Fourier transform infrared (DSC-FTIR) combined system to simultaneously investigate the thermal-induced intramolecular cyclization or polymorphic interconversion processes of many drugs [40-43]. Moreover, the simultaneous formation and detection of several co-crystals in the solid state had been successfully performed by this unique technique via a one-step procedure [44-48]. This powerful DSC-FTIR technique is a simple, quick, and timesaving

tool, and can one-step establish the correlation between the thermal response and the informative IR spectra of structural changes of the sample. Here, Soluplus was selected as a polymeric carrier and IMS was chosen as a model drug. The aim of this study was attempted to simultaneously prepare and examine the amorphous formation of IMC in the IMC/Soluplus mixture in real-time by using this DSC-FTIR combined system as an accelerated method.

Materials and Methods

Materials

Indomethacin (IMC, γ-form) was purchased from Sigma-Aldrich Chemical Co. (St. Louis, Missouri, USA), which was confirmed by FTIR microspectroscopy and directly used without further treatment. Soluplus® was kindly obtained from BASF Co., Ltd. (Ludwigshafen, Germany). All organic solvents used were reagent grade. Potassium bromide (KBr) crystals were bought from Jasco Co. (Tokyo, Japan).

Preparation of α-IMC and amorphous IMC

The α-form of IMC (α-IMC) was prepared by dissolving γ-IMC in the heated absolute ethanol and precipitated with water at room temperature, according to our previous studies [46,49]. While amorphous IMC was prepared by melting IMC at 161°C for isothermal 5 min and quench cooling in liquid nitrogen [49-50]. Both samples were stored in a desiccator filled with anhydrous calcium chloride.

Preparation of γ-IMC/Soluplus physical mixture with or without solvent evaporation

A γ-IMC/Soluplus physical mixture with the same weight ratio of γ-IMC and Soluplus was previously weighed, and then mixed well in the mortar and pestle. Another γ-IMC/Soluplus physical mixture (weight ratio = 1:1) was previously dissolved in acetone, and then evaporated under about 50°C on a hot plate. Soluplus alone was also dissolved in acetone and evaporated under the same process. Until all the evaporated samples were completely dried, and then stored in a desiccator filled with anhydrous calcium chloride for further studies.

Identification of different samples

About 8~10 mg of each sample was respectively analyzed by DSC (DSC, Q 20, TA Instruments, Inc., New Castle, DE, USA) at a heating rate of 3°C/min with an open pan system in a stream of N_2 gas over a temperature range of 30-250°C. The instrument was calibrated for temperature and heat flow using indium as the standard. Moreover, a trace amount of sample was sealed inside two KBr pellets (without any grinding process with KBr powders) by direct compression with an IR spectrophotometric hydraulic press (Riken Seiki Co., Tokyo, Japan) at 400 kg/cm^2 for 15s. The compressed KBr disc was examined by transmission FTIR microspectroscopy (IRT-5000-16/FTIR-6200, Jasco Co., Tokyo, Japan) with a mercury-cadmium telluride (MCT) detector. All the FTIR spectra were generated by compiling a series of 256 interferograms collected at 4 cm^{-1} resolution and at 100 scans [44-48].

Simultaneous DSC–FTIR microspectroscopic investigations

Each sample was sealed again into two pieces of KBr pellets, similar to the above procedure. Each compressed KBr disc containing differed sample was directly placed onto a micro hot stage (DSC microscopy cell, FP 84, Mettler, Greifensee, Switzerland). This DSC microscopy cell was then set in an FTIR microspectroscope (IRT-5000-16/FTIR-6200, Jasco). The temperature of the DSC microscopy cell was monitored with a central processor (FP 80 HT, Mettler, Greifensee, Switzerland). Each sample disc was previously equilibrated to the starting temperature (30°C) and then heated from 30°C to 170°C for γ-IMC, to 200°C for amorphous IMC, or to 250°C for Soluplus samples with or without mixing with γ-IMC at a heating rate of 3°C/min under ambient conditions. At the same time, the thermal-responsive IR spectra were simultaneously recorded in the course of heating process. The operation was performed in the transmission mode [44-48]. This DSC-FTIR combined system was carried out with a non-isothermal method by two consecutive heating-cooling cycles.

Results and Discussion

Identification of different samples

The DSC curve of raw material of γ-IMC and α-IMC prepared were determined by DSC analytical technique. Two endothermic peaks at 161 and 156°C are respectively observed in the DSC curve (Figure 1A-a and b), which were separately attributed to the fusion of γ-IMC

and α-IMC [32, 49-50]. On the other hand, the DSC curve of the amorphous IMC (Figure 1A-c) displays one exothermic peak at 123°C and three endothermic peaks at 44, 156 and 161°C. The exothermic peak at 123°C was due to the recrystallization of the amorphous IMC after pass through the *Tg* at 44oC, and another two endothermic peaks at 156°C and 161°C were attributed to the fusion of α-IMC and γ-IMC, respectively. This Tg value near 44°C was consistent with the *Tg* values of amorphous IMC previously reported at 41.25 ± 1.16°C and 43.0 ± 0.4°C [33,51]. From the DSC data, the amorphous IMC first exhibited an endothermic relaxation peak near at 44°C corresponding to glass transition, which was accompanied by exothermic recrystallization, and followed by transformation into α-IMC and less often into γ-IMC. This reveals that the amorphous form of IMC was easily prepared by quench cooling of the melt. While the DSC thermogram of pure Soluplus shows a broad endothermic peak at 73˚C (Figure 2A-d), which was belonged to *Tg* of amorphous Soluplus [22-23,52]. When Soluplus was previously dissolved in acetone and then evaporated, the DSC curve of the acetone-evaporated Soluplus was similar to that of the DSC thermogram of pure Soluplus, suggesting that the solvent evaporation process did not influence the amorphous structure of Soluplus.

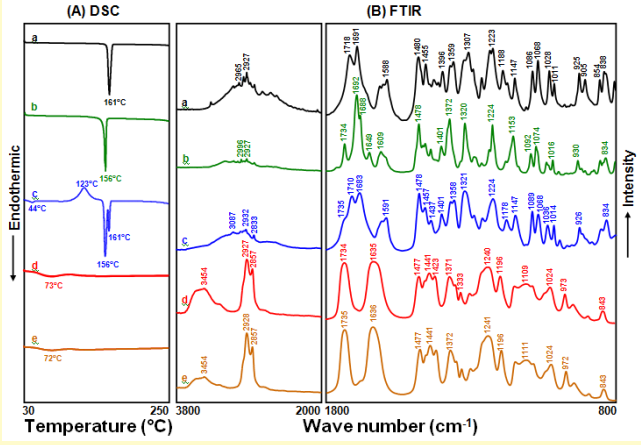

Figure 1: *DSC curves and FTIR spectra of γ-IMC (a), α-IMC (b), amorphous IMC (c), pure Soluplus (d) and the acetone-evaporated Soluplus (e) samples.*

Figure 1B indicates the FTIR spectra of γ-IMC (a), α-IMC (b), amorphous IMC (c), pure Soluplus (d) and the acetone-evaporated Soluplus (e) samples. The FTIR data clearly reveals several characteristic IR absorption bands and their assignments of γ-IMC and α-IMC as follows (in cm^{-1}): 1718 [ν(C = O) of carboxylic acid dimer], 1691 [benzoyl ν(C = O)], 1625–1575 and 1480 (C = C of aromatic rings), 1307 (C–O of acidic group), 1270–1200 (-C-O stretching, ether group), 1068 (C–Cl) for γ-IMC [49-53]; 1734 [non-hydrogen bonded acid ν(C = O)], 1692 [benzoyl ν(C = O)], 1688 and 1649 [hydrogen bonded acid ν(C = O)], 1478 (C = C of aromatic rings), 1320 (C-O of acidic group), 1224 (-C-O stretching, ether group), and 1074 (C–Cl) for α-IMC [49-53].

The amorphous IMC exhibits a unique FTIR spectrum including a shoulder at 1735 cm^{-1} [non-hydrogen bonded acid ν(C = O)], 1710 cm^{-1} [asymmetric acid ν(C = O) of a cyclic dimer], 1683 cm^{-1} [benzoyl ν(C = O)], 1591 cm^{-1} [ring vibration of indole], which was markedly different from that of the pure γ-IMC or α-IMC between 1750 and 1550 cm^{-1} and was in agreement with the reported IR spectrum of amorphous IMC [49-53]. The band at 1718 cm^{-1} due to asymmetric acid ν(C = O) of a cyclic dimer for crystalline γ-IMC was shifted to a lower frequency of about 1710 cm^{-1}, implying that the dimers formation was also presented in the amorphous state of IMC [50-51]. Whereas the characteristic IR absorption bands and their assignments for pure Soluplus and acetone-evaporated Soluplus are listed as follows: around 3350-3650 cm^{-1} [intermolecular hydrogen bonded -OH stretching]; 2927 and 2857 cm^{-1} [asymmetric and symmetric CH stretching]; 1734 (1735) cm^{-1} [ester carbonyl stretching]; 1635 (1636) cm^{-1} [tertiary amide C = O stretching]; 1477 cm^{-1} [C-O-C stretching]; 1441 cm^{-1} [CH3 bending]; 1240 (1241) and 1109 (1111) cm^{-1} [ester C–O stretching], respectively [23, 52, 54]. There was no any change in the FTIR spectra for Soluplus with or without acetone treatment.

Thermal-induced structural transformation of IMC polymorphs studied by DSC-FTIR microspectroscopy

The conformational and thermal changes in the phase transition of γ-IMC and amorphous IMC samples were directly estimated by DSC-FTIR microspectroscopy. A three-dimensional FTIR plot of γ-IMC as a function of temperature is shown in Figure 2. The thermal-dependent changes in peak intensity for several specific bands are also displayed. The thermal-dependent IR spectral contour and peak intensities of γ-IMC were clearly altered around 154°C, close to an onset temperature of melting point at 161°C for γ-IMC in the DSC curve. Below 154°C, this three-dimensional FTIR spectral map maintained a nearly constant contour. However, the peaks assigned to the C = O stretching for both the carboxylic and benzoyl groups (1500-1800 cm^{-1}) in IMC structure were substantially changed beyond 154°C. With the increase of temperature, the peak at 1718 cm^{-1} was gradually shifted to 1714 cm^{-1}. Moreover, a new peak at 1741 cm^{-1} was also markedly observed, which might be attributed to the dissociation of hydrogen-bonded carboxylic cyclic dimers in γ-IMC structure (1718 cm^{-1}) to form the non-hydrogen bonded acid monomer of γ-IMC (1741 cm^{-1}) at higher temperatures [50-55]. Furthermore, the peak at 1308 cm^{-1} (C-O of acidic groups) also exhibited a similar thermal shift to 1317 cm^{-1}. The peaks at 1360 and 1188 cm^{-1} were also shifted to 1352 and 1176 cm^{-1}, respectively. Many specific band intensities for γ-IMC were suddenly changed as the temperature exceeded 154°C by DSC analysis.

Fig. 2

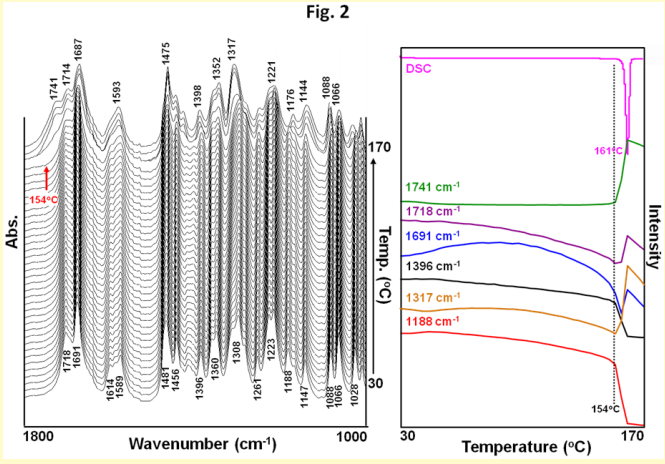

Figure 2: *Three-dimensional FTIR plot of γ-IMC as a function of temperature by DSC-FTIR combined system and the thermal-dependent changes in peak intensity for several specific bands.*

Figure 3 displays the three-dimensional FTIR results of amorphous IMC measured by the simultaneous DSC-FTIR method. It is evident that the thermal-related changes in IR peak intensity for several specific spectra were clearly observed. These spectral changes significantly differed from that of the spectral changes for γ-IMC. Obviously, four marked changes in the IR peak intensities were observed in the three-dimensional contour profile. However, there were no substantial changes in the contour profile before 99°C. Once the temperature was beyond 99°C, all the IR peak intensities were slightly decreased at initial and then markedly reduced as the temperature was increased from 114°C to 132°C. Beyond 132°C, all the IR spectral peaks became broader and less intense. However, the sharp IR peak intensities reappeared at temperatures > 152°C. The multiple broad IR peaks within 132°C-152°C might be due to the fusion of the recrystallized IMC. The sharp IR peak intensities above 152°C should be corresponded to the phase transformation from the molten IMC to α-IMC and γ-IMC. The reappearance of the sharp IR peaks at 1741 and 1714 cm^{-1} can explain this phenomenon, similar to the results of Figure 2 at higher temperatures. In addition, the changes in several specific IR peak intensities with temperature also confirm this spectral contour profile.

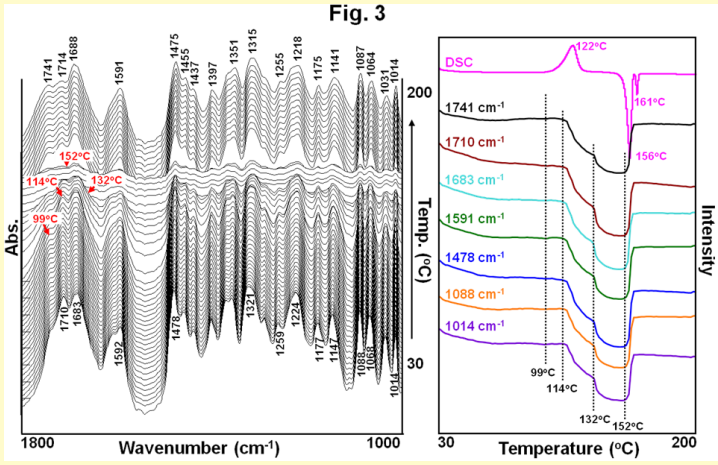

Figure 3: *Three-dimensional FTIR plot of amorphous IMC as a function of temperature by DSC-FTIR combined system and the thermal-dependent changes in peak intensity for several specific bands.*

Thermal-induced amorphous IMC formation in the γ-IMC/Soluplus physical mixture studied by DSC-FTIR microspectroscopy using alternate heating/cooling cycles

Figure 4 shows a DSC-FTIR data in which a Soluplus alone was heated, cooled and then reheated at a heating rate of 3°C/min under ambient conditions. In Figure 4A, it clearly indicates that both IR peaks at 1734 and 1635 cm^{-1} assigned to the ester C = O and tertiary amide C = O stretching vibrations of Soluplus were shifted to 1738 and 1643 cm^{-1} at higher temperatures in the first-heating run. The spectral shifts in the FTIR spectra were due to the dissociation of hydrogen bonding within the molten Soluplus structures at higher temperatures. Once the molten Soluplus was cooled to room temperature, its IR peaks at higher wave number were quickly returned to the original lower peak position. Since Soluplus is amorphous in nature and has high molecular weight, the molten Soluplus was quickly returned to its native amorphous state with unique IR peaks at 1735 and 1635 cm^{-1} after cooling (Figure 4B). After the first heating-cooling cycle, Soluplus shows more consistent and sharp three-dimensional FTIR spectral contour map after the second-heating run, as shown in Figure 4B.

Figure 5 reveals the three-dimensional FTIR spectral plots of the γ-IMC/Soluplus physical mixture with the same weight ratio via two consecutive heating-cooling-heating cycles. It clearly indicates that several IR peaks at 1735, 1635, 1479, 1441, 1423 and 1371 cm^{-1} corresponded to the Soluplus and at 1717, 1692, 1479 and 1455 cm^{-1} assigned to the γ-IMC were presented in the FTIR spectra of γ-IMC/Soluplus physical mixture at the initial temperature, suggesting that both components of γ-IMC and Soluplus were coexisted in the physical mixture (Figure 5A). In the first-heating run, the first-heated sample shows the marked changes in the FTIR spectral map, particularly in the 1800-1500 cm^{-1} region (Figure 5A). It is evident that several IR spectral changes and shifts from 97, 157, 162 and 185°C were observed. In particular, the IR peaks at 1717 and 1692 cm^{-1} assigned to the γ-IMC disappeared but four new peaks at 1738, 1687, 1643 and 1604 cm^{-1} were observed in the IR spectra of the 250°C-heated sample. After cooling to room temperature, four IR peaks at 1734, 1682, 1637 and 1594 cm^{-1} shifted from 1738, 1687, 1643 and 1604 cm^{-1} were obtained (Figure 5B). Both IR peaks at 1734 and 1637 cm^{-1} were attributed to the Soluplus and at 1682 and 1594 cm^{-1} were corresponded to the formation of amorphous IMC, as compared with Figure 1. This strongly implies that the γ-form of IMC in the γ-IMC/Soluplus physical mixture was gradually dissociated its hydrogen-bonding in cyclic dimers in the polymeric blends with Soluplus via the first-heating run by DSC-FTIR combined system. After the first heating-cooling cycle, the formation of IMC/Soluplus ASD system had been successfully produced due to the appearance of both characteristic IR peaks at 1682 and 1594 cm^{-1} for the amorphous IMC formed. In addition, Figure 5B also shows the consistent contour map for three-dimensional FTIR spectra of the first-heated IMC/Soluplus sample in the second-heating run, since the first-heated IMC/Soluplus sample had been completely transformed to an IMC/Soluplus ASD system.

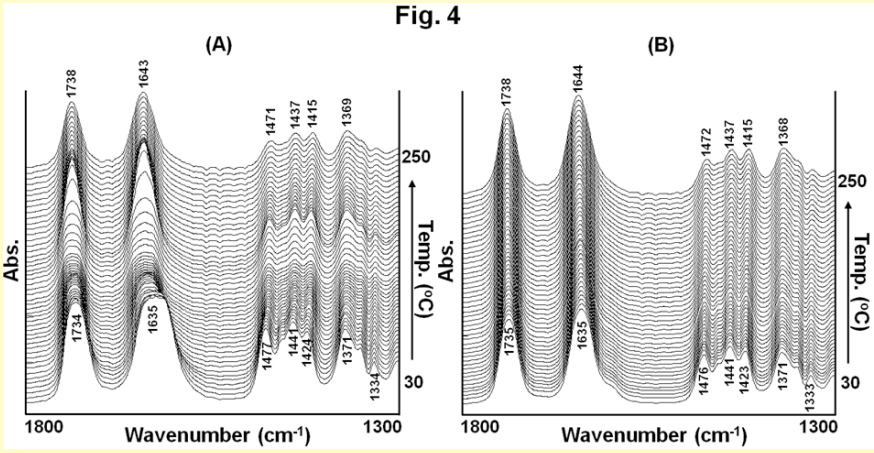

Figure 4: *Three-dimensional FTIR plots of pure Soluplus as a function of temperature by DSC-FTIR combined system via alternate heating/cooling cycles.*

Key: *A, first-heating process; B, second-heating process*

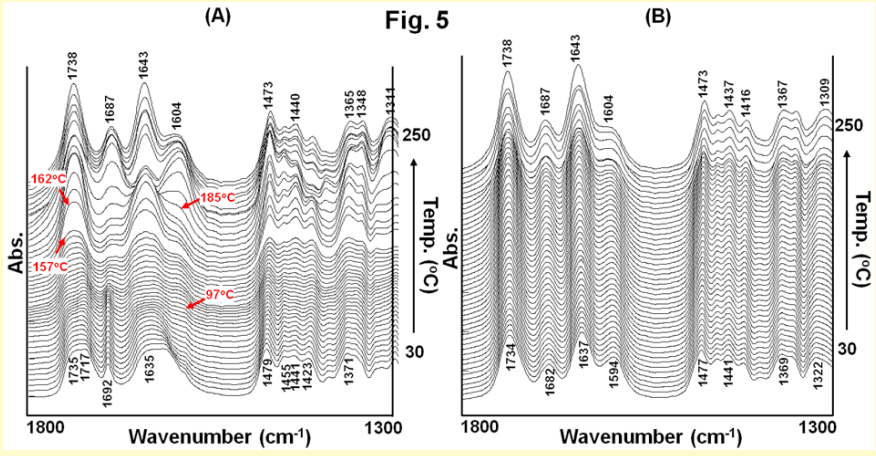

Figure 5: *Three-dimensional FTIR plot of γ-IMC/Soluplus physical mixture with the same weight ratio as a function of temperature by DSC-FTIR combined system via alternate heating/cooling cycles.*

Key: *A, first-heating process; B, second-heating process.*

Figure 6 displays the comparisons of FTIR spectra of the γ-IMC/Soluplus physical mixture before and after different heating-cooling-heating treatments. Obviously, the appearance of two IR peaks at 1687 and 1604 cm^{-1} due to the dissociation of hydrogen-bonding of the cyclic dimers in γ-IMC structure for the molten IMC/Soluplus blends at higher temperature via the first-heating run (Figure 6b). After cooling the molten sample to room temperature, the IR peaks at 1682 and 1594 cm^{-1} for the amorphous IMC formed in the IMC/Soluplus ASD system were observed (Figure 6c). By reheating the IMC/Soluplus ASD system, the same FTIR spectrum as Figure 6b was also obtained (Figure 6d). From the results of Figures 5 and 6, it strongly implies that simultaneous DSC-FTIR combined system was not only capable of producing the IMC/Soluplus ASD system from physical mixture but also capable of determining the amorphous formation of IMC in the IMC/Soluplus ASD system in real-time via a one-step procedure.

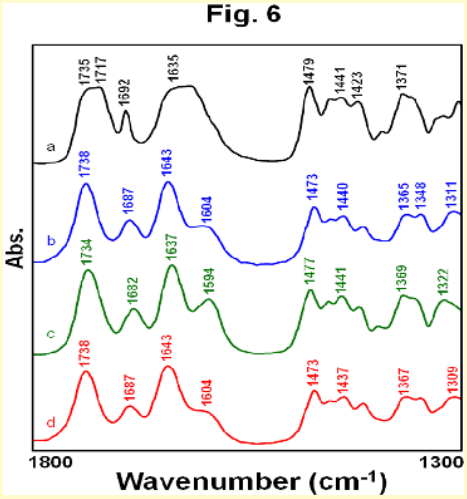

Figure 6: *Comparisons of FTIR spectra of γ-IMC/Soluplus physical mixture with the same weight ratio at different heating or cooling temperatures via alternate heating/cooling cycles.*
Key: *a, at 30°C; b, at 250°C; c, cooled to 30°C; d, re-heating to 250°C.*

Similar DSC-FTIR spectral contour profiles were obtained for the γ-IMC/Soluplus physical mixture after acetone evaporation at 50°C on a hot plate. Figure 7 shows the three-dimensional FTIR spectral plots of the acetone-evaporated IMC/Soluplus mixture through two consecutive heating-cooling-heating cycles. Obviously, both three-dimensional FTIR spectral contour maps obtained from first- and second-heating runs were similar, due to the formation of IMC/Soluplus ASD system already prepared after solvent evaporation. The IR peaks at 1735 (1734) and 1635 (1636) cm^{-1} were assigned to the Soluplus, while the IR peaks at 1682 and 1594 cm-1 were corresponded to the amorphous IMC, respectively, suggesting the amorphous IMC being existed within the IMC/Soluplus ASD system. Once the amorphous IMC was formed in the IMC/Soluplus ASD system, there was less change in the three-dimensional FTIR spectral contour map for this solid dispersion after repeating heating-cooling runs.

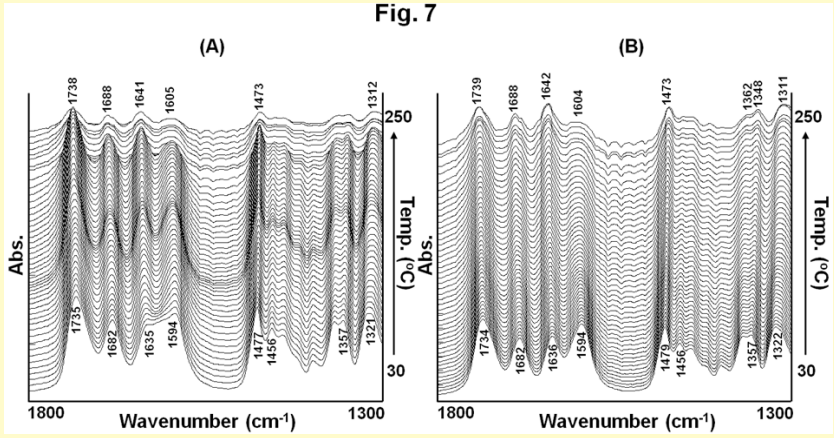

Figure 7: *Three-dimensional FTIR plot of acetone-evaporated γ-IMC/Soluplus physical mixture with the same weight ratio as a function of temperature by DSC-FTIR combined system via alternate heating/cooling cycles.*
Key: *A, first-heating process; B, second-heating process*

Conclusion

The present study clearly indicates that the unique DSC–FTIR technique could be used to simultaneously produce and detect the amorphous formation of IMC in the IMC/Soluplus ASD system in real-time.

Conflict of interest

The authors declare that there is no conflict of interest.

Acknowledgements

This work was supported by Ministry of Science and Technology, Taipei, Taiwan, ROC (MOST 103-2320-B-264-002-MY2).

Bibliography

1. Avdeef A. "Absorption and drug development: Solubility, permeability, and charge state". 2nd Ed., Hoboken, New Jersey, John Wiley & Sons (2003).
2. Kerns EH. "High throughput physicochemical profiling for drug discovery". *Journal of Pharmaceutical Sciences* 90.11 (2001): 1838-1858.
3. Amidon GL., *et al*. "A theoretical basis for a biopharmaceutic drug classification: the correlation of in vitro drug product dissolution and in vivo bioavailability". *Pharmaceutical Research* 12.3 (1995): 413-420.
4. Benet LZ. "The role of BCS (biopharmaceutics classification system) and BDDCS (biopharmaceutics drug disposition classification system) in drug development". *Journal of Pharmaceutical Sciences* 102.1 (2013): 34-42.
5. Buckley ST., *et al*. "Biopharmaceutical classification of poorly soluble drugs with respect to enabling formulations". *European Journal of Pharmaceutical Sciences* 50.1 (2013): 8-16.
6. Kwok PC and HK Chan. "Nanotechnology versus other techniques in improving drug dissolution". *Current Pharmaceutical Design* 20.3 (2014): 474-482.
7. Kawabata Y., *et al*. "Formulation design for poorly water-soluble drugs based on biopharmaceutics classification system: basic approaches and practical applications". *International Journal of Pharmaceutics* 420.1 (2011): 1-10.
8. Kumar S., *et al*. "Drug carrier systems for solubility enhancement of BCS class II drugs: a critical review". *Critical Reviews in Therapeutic Drug Carrier Systems* 30.3 (2013): 217-256.
9. Guo P. "Amorphous pharmaceutical solids: characterization, stabilization, and development of marketable formulations of poorly soluble drugs with improved oral absorption". *Molecular Pharmaceutics* 5.6 (2008): 903-904.
10. Vasconcelos T., *et al*. "Solid dispersions as strategy to improve oral bioavailability of poor water soluble drugs". *Drug Discovery Today* 12.23 (2007): 1068-1075.
11. Vo CL., *et al*. "Current trends and future perspectives of solid dispersions containing poorly water-soluble drugs". *European Journal of Pharmaceutics and Biopharmaceutics* 85.3 (2013): 799-813.
12. Shah N., *et al*. "Amorphous Solid Dispersions: Theory and Practice". Springer-Verlag, New York (2014).
13. Kavanagh A., *et al*. "Developing amorphous pharmaceuticals: Opportunity and necessity". *American Pharmaceutical Review* 15.4 (2012).
14. Shalaev E and G Zografi. "The concept of 'structure' in amorphous solids from the perspective of the pharmaceutical sciences". In, *Levine H. Amorphous Food and Pharmaceutical Systems*. Cambridge: The Royal Society of Chemistry (2002): 11-30.
15. Lee TW., *et al*. "Delivery of poorly soluble compounds by amorphous solid dispersions". *Current Pharmaceutical Design* 20.3 (2014): 303-324.
16. Laitinen R., *et al*. "Emerging trends in the stabilization of amorphous drugs". *International Journal of Pharmaceutics* 453.1 (2013): 65-79.
17. Meng F., *et al*. "Classification of solid dispersions: correlation to (i) stability and solubility (ii) preparation and characterization techniques". *Drug Development and Industrial Pharmacy* (2015): 1-15.

18. Van den Mooter G. "The use of amorphous solid dispersions: A formulation strategy to overcome poor solubility and dissolution rate". *Drug Discovery Today Technology* 9.2 (2012): 71-174.
19. Tian Y., *et al*. "An investigation into the role of polymeric carriers on crystal growth within amorphous solid dispersion systems". *Molecular Pharmaceutics* 12.4 (2015): 1180-1192.
20. Enose AA., *et al*. "Formulation and characterization of solid dispersion prepared by hot melt mixing: A fast screening approach for polymer selection". *Journal of Pharmaceutics* 2014 (2014): Article ID 105382.
21. Van Eerdenbrugh B and LS Taylor. "Small scale screening to determine the ability of different polymers to inhibit drug crystallization upon rapid solvent evaporation". *Molecular Pharmaceutics* 7.4 (2010): 1328-1337.
22. Reintjes T. "Solubility enhancement with BASF pharma polymers: Solubilizer compendium". *BASF SE Pharma Ingredients & Services* October, 2011.
23. Shamma RN and M Basha. "Soluplus: A novel polymeric solubilizer for optimization of carvedilol solid dispersions: Formulation design and effect of method of preparation". *Powder Technology* 237.3 (2013): 406-414.
24. Nagy ZK., *et al*. "Comparison of electrospun and extruded Soluplus-based solid dosage forms of improved dissolution". *Journal of Pharmaceutical Sciences* 101.1 (2012): 322-332.
25. Hardung H., *et al*. "Combining HME & solubilization: Soluplus - The solid solution". *Drug Delivery Technology* 10.3 (2010): 20-27.
26. Teja SB., *et al*. "Drug–excipient behavior in polymeric amorphous solid dispersions". *Journal of Excipients and Food Chemicals* 4.3 (2013): 70-94.
27. Linn M., *et al*. "Soluplus as an effective absorption enhancer of poorly soluble drugs *in vitro* and *in vivo*". *European Journal of Pharmaceutical Sciences* 45.3 (2012): 336-343.
28. Swift GL., *et al*. "Risk of ulceration with long-term indomethacin: endoscopic and histological changes in upper gastro-intestinal mucosa". *Digestion* 53.1-2 (1992): 88-93.
29. Ackerstaff E., *et al*. "Antiinflammatory agent indomethacin reduces invasion and alters metabolism in a human breast cancer cell line". *Neoplasia* 9.3 (2007): 222-235.
30. Qin S., *et al*. "Indomethacin induces apoptosis in the EC109 esophageal cancer cell line by releasing second mitochondria-derived activator of caspase and activating caspase-3". *Molecular Medicine Reports* 11.6 (2015): 4694-4700.
31. ElShaer A., *et al*. "Use of amino acids as counterions improves the solubility of the BCS II model drug, indomethacin". *Current Drug Delivery* 8.4 (2011): 363-372.
32. Pan X., *et al*. "Increasing the dissolution rate of a low-solubility drug through a crystalline-amorphous transition: a case study with indomethacin". *Drug Development and Industrial Pharmacy* 34.2 (2008): 221-231.
33. Greco K and R. Bogner. "Crystallization of amorphous indomethacin during dissolution: effect of processing and annealing". *Molecular Pharmaceutics* 7.5 (2010): 1406-1418.
34. Andronis V and G Zografi. "Crystal nucleation and growth of indomethacin polymorphs from the amorphous state". *Journal of Non-Crystalline Solids* 271.3 (2000): 236-248.
35. Patterson JE., *et al*. "The influence of thermal and mechanical preparative techniques on the amorphous state of four poorly soluble compounds". *Journal of Pharmaceutical Sciences* 94.9 (2005): 1998-2012.
36. Savolainen M., *et al*. "Screening for differences in the amorphous state of indomethacin using multivariate visualization". *European Journal of Pharmaceutical Sciences* 30.2 (2007): 113-123.
37. Maniruzzaman M., *et al*. "A Review of Hot-Melt Extrusion: Process Technology to Pharmaceutical Products" *ISRN Pharmaceutics* 2012 (2012): Article ID 436763.
38. Repka MA., *et al*. "Melt Extrusion: Materials, Technology and Drug Product Design". *Springer* 2013.
39. Thiry J., *et al*. "A review of pharmaceutical extrusion: critical process parameters and scaling-up". *International Journal of Pharmaceutics* 479.1 (2015): 227-240.
40. Hsu CH and SY Lin. "Rapid examination of the kinetic process of intramolecular lactamization of gabapentin using DSC–FTIR". *Thermochimica Acta* 486.1 (2009): 5-10.

41. Lin SY., *et al*. "DSC–FTIR microspectroscopy used to investigate the thermal-induced Intramolecular cyclic anhydride formation between Eudragit E and PVA copolymer". *Polymer Journal* 43.6 (2011): 577-580.
42. Wang SL., *et al*. "A continuous process for solid-state dehydration, amorphization and recrystallization of metoclopramide HCL monohydrate studied by simultaneous DSC–FTIR microspectroscopy". *Journal of Thermal Analysis and Calorimetry* 104.1 (2011): 261-264.
43. Lin SY and SL Wang. "Advances in simultaneous DSC–FTIR microspectroscopy for rapid solid-state chemical stability studies: some dipeptide drugs as examples". *Advanced Drug Delivery Reviews* 64.5 (2012): 461-478.
44. Wu TK., *et al*. "Simultaneous DSC–FTIR microspectroscopy used to screen and detect the co-crystal formation in real time". *Bioorganic & Medicinal Chemistry Letters* 21.10 (2011): 3148-3151.
45. Lin HL., *et al*. "The ophylline-citric acid co-crystals easily induced by DSC-FTIR microspectroscopy or different storage conditions". *Asian Journal of Pharmaceutical Sciences* 8.1 (2013): 19-27.
46. Lin HL., *et al*. "An investigation of indomethacin/nicotinamide co-crystal formation induced by thermal stress in the solid or liquid state". *Journal of Pharmaceutical Sciences* 103.8 (2014): 2386-2395.
47. Lin HL., *et al*. "Screening and characterization of cocrystal formation of metaxalone with short-chain dicarboxylic acids induced by solvent-assisted grinding approach" *Thermochimica Acta* 575 (2014): 313-321.
48. Lin HL., *et al*. "Real-time co-crystal screening and formation between indomethacin and saccharin via DSC analytical technique or DSC-FTIR microspectroscopy". *Journal of Thermal Analysis and Calorimetry* 120 (2015): 679-687.
49. Kao CY., *et al*. "Thermo analytical and spectroscopic studies on amorphization and phase transition of amorphous indomethacin prepared by two melt-cooling processes". *ScienceJet* 4 (2015): 148.
50. Taylor LS and G Zografi. "Spectroscopic characterization of interactions between PVP and indomethacin in amorphous molecular dispersions". *Pharmaceutical Research* 14.12 (1997): 1691-1698.
51. Karmwar P., *et al*. "Investigation of properties and recrystallisation behaviour of amorphous indomethacin samples prepared by different methods". *International Journal of Pharmaceutics* 417.1-2 (2011): 94-100.
52. Terife G., *et al*. "Hot melt mixing and foaming of Soluplus and Indomethacin". *Polymer Engineering & Science* 52 (2012): 1629-1639.
53. Wang F., *et al*. "Oxidized mesoporous silicon microparticles for improved oral delivery of poorly soluble drugs". *Molecular Pharmaceutics* 7.1 (2010): 227-236.
54. Thakral NK., *et al*. "Soluplus--solubilized citrated camptothecin-a potential drug delivery strategy in colon cancer". *AAPS PharmSciTech* 13 (2012): 59-66.
55. Tong P and G Zografi. "A study of amorphous molecular dispersions of indomethacin and its sodium salt". *Journal of Pharmaceutical Sciences* 90.12 (2001): 1991-2004.

Volume 2 Issue 1 September 2015